



## Kinetic models comparison for steam gasification of coal/biomass blend chars



Chaofen Xu<sup>a</sup>, Song Hu<sup>a,\*</sup>, Jun Xiang<sup>a</sup>, Haiping Yang<sup>a</sup>, Lushi Sun<sup>a</sup>, Sheng Su<sup>a</sup>, Baowen Wang<sup>b</sup>, Qindong Chen<sup>a</sup>, Limo He<sup>a</sup>

<sup>a</sup>State Key Laboratory of Coal Combustion, Huazhong University of Science and Technology, Wuhan 430074, China

<sup>b</sup>College of Electric Power, North China University of Water Conservancy and Hydroelectric Power, Zheng Zhou 450011, China

### HIGHLIGHTS

- The most synergistic interaction occurred at the mass ratio of SD to LN as 1:4.
- RPM model was identified as best for steam-gasification of SD and LN blends.
- Rational kinetic parameters were reached.

### ARTICLE INFO

#### Article history:

Received 30 May 2014

Received in revised form 23 July 2014

Accepted 24 July 2014

Available online 20 August 2014

#### Keywords:

Coal

Biomass

Co-gasification

Gas–solid kinetic models

### ABSTRACT

The non-isothermal thermogravimetric method (TGA) was applied to different chars produced from lignite (LN), sawdust (SD) and their blends at the different mass ratios in order to investigate their thermal reactivity under steam atmosphere. Through TGA analysis, it was determined that the most prominent interaction between sawdust and lignite occurred at the mass ratio of sawdust/lignite as 1:4, but with further dose of more sawdust into its blends with lignite, the positive interaction deteriorated due to the agglomeration and deactivation of the alkali mineral involved in sawdust at high steam gasification temperature. Through systematic comparison, it could be observed that the random pore model was the most suitable among the three gas–solid reaction models adopted in this research. Finally, rational kinetic parameters were reached from these gas–solid reaction models, which provided a basis for design and operation of the realistic system of co-gasification of lignite and sawdust in this research.

© 2014 Elsevier Ltd. All rights reserved.

## 1. Introduction

Biomass is regarded as renewable and inexpensive natural resources. And its efficient and massive utilization should be one of the rational options to substitute the traditional fossil fuels to meet the increasing energy demand from the society, and simultaneously to reduce emission of various hazardous pollutions such as SO<sub>x</sub>, NO<sub>x</sub> etc. as well as to inhibit greenhouse effect by decrease of CO<sub>2</sub> emission. Of course, there also existed many disadvantages with biomass energy utilization, such as large volume of biomass resources, outdated, small-scale and low efficiency of biomass energy utilization technology. Therefore, it would be meaningful to co-utilize coal and biomass, e.g. co-gasification of coal and biomass will receive trade-off between solely utilization of coal

or biomass, and efficiently solve the energy demand from the society and atmospheric pollution as accompanied (Edreis et al., 2014; Xu et al., 2014). As such, co-gasification technology has attracted enough attention and received intensive research.

Reactivity of different coal and biomass changed greatly. And co-gasification behavior of coal and biomass was far different from single gasification of coal or biomass involved, which would result in various difficulties in design and operation of the realistic co-gasification utility. Considering the widespread distribution of coal and biomass resources and there different reaction behavior, it is necessary to conduct more in-depth research on the co-gasification of typical coal and biomass models.

Determination of reaction kinetic parameters is very important to acquire the full knowledge on co-gasification of coal and biomass. As a typical inhomogeneous gas–solid reaction, co-gasification of coal and biomass has been extensively investigated with various gas–solid reaction kinetic models. But due to inhomogeneous component structure of coal and biomass and their complicated

\* Corresponding author. Tel.: +86 27 87542417; fax: +86 27 87545526.

E-mail addresses: [husong\\_hust@hotmail.com](mailto:husong_hust@hotmail.com) (S. Hu), [yhp2002@163.com](mailto:yhp2002@163.com) (H. Yang).

gasification behavior, their gasification kinetic parameters acquired from typical gas–solid kinetic models differed greatly.

Even for the same coal or biomass under the same gasification condition, their kinetic parameters reached from different gas–solid kinetic models were also not identical. On the one hand for simulated investigator of gasification of only coal, [Everson et al. \(2008\)](#) investigated gasification of char produced from six kinds of Chinese anthracites and two kinds of high-ash coal using the shrinking core model (SCM) and the simulation results reached were satisfactory. [Wu et al. \(2006\)](#) compared the simulated results of steam-gasification of Yanzhou bituminous coal char from both homogeneous reaction model (HRM) and SCM and pointed out the results from SCM was better. But [Fermoso et al. \(2008\)](#) simulated steam-gasification of coal chars from five different ranked coals using three different typical gas–solid reaction kinetic models, including HRM, SCM and random pore model (RPM), and found out that RPM was superior to those other gas–solid models. On the other hand, many workers have also simulated biomass only ([Ahmed and Gupta, 2009](#); [Kajitani et al., 2006](#); [Liu et al., 2008](#)). But, simultaneous simulated investigation of co-gasification of coal and different biomass were quite limited. Therefore, it is also of great necessity to simulated investigating co-gasification of coal and biomass.

In this research, non-isothermal steam co-gasification of one typical Chinese coal and two kinds of biomass were systematically investigated using thermogravimetric method (TGA). Furthermore, their co-gasification behavior under the steam atmosphere was simulated using three typical gas–solid kinetic models, including SCM, HRM and RPM. And the kinetic parameters inherent in the co-gasification of the selected coal and biomass were reached; the most suitable model was determined to simulate the steam co-gasification of the selected coal and biomass in this research.

## 2. Methods

### 2.1. Samples

The raw materials used in this work were one kind of typical Chinese lignite from Inner Mongolia, China (designated as LN) and a type of biomass, i.e. sawdust (designated as SD), which was collected from Hubei province, China with a high volatile content. These materials were ground, sieved and the resulting fractions between 150 and 180  $\mu\text{m}$  was collected for the gasification tests. The volatile matter contents of the raw samples were 35.15

and 79.45 wt.% (dry basis) for lignite and sawdust, respectively. Furthermore, ashes of the raw lignite coal and raw sawdust biomass were prepared as followed. As to lignite, its ash was prepared according to Chinese National Standard (GB/T 212-2001) and heated in the muffle furnace from the ambient to 815 °C with hold time for one hour, while for sawdust biomass, its ash was conducted by ASTM E870-82 as suggested by [Wang et al. \(2011\)](#) and its final ashing temperature was only 600 °C in avoidance of the inherent mineral vaporization. And the chemical composition of ashes of both samples is listed in [Table 1](#).

### 2.2. Char preparation

The chars were prepared by devolatilization of the raw fuels on the tube pipe furnace with the diameter of 20 mm.  $1.0 \pm 0.05$  g the raw fuels are loaded into quartz sieve basket and the basket is placed in the cool zone of the reactor. Nitrogen gas flow (purity > 99.999%, flow rate of 600 ml/min) heated by the preheater is inlet into reactor to remove any air from the system and provide an inert atmosphere until the quartz reactor is heated to the desired temperature of 900 °C. When the desired temperature is attained and remains constant, the sample is quickly pushed into center heating zone of reactor to pyrolysis and held at this temperature for 20 min. Afterwards, the chars were cooled down under a flow of nitrogen to room temperature.

The char samples were ground and sieved to a size <150  $\mu\text{m}$  for the gasification experiments. The samples are tested by five blended coal-to-biomass mass ratios as 1:0; 4:1; 1:1; 1:4 and 0:1, respectively. Proximate analysis and ultimate analyses of the char samples were carried out using TGA-2000 (Las Navas Instruments, Spain) and EL-2 analyzer (Vario Company, Germany) elemental analyzer, respectively ([Long et al., 2012](#)). The results are given in [Table 2](#) below.

### 2.3. Co-gasification tests

Thermogravimetric analysis is frequently used to determine the kinetic parameters of carbonaceous fuels ([Arenillas et al., 2004](#); [Barkia et al., 2006](#); [Elbeyli and Piskin, 2006](#)). In this work, the reaction kinetics of the coal and biomass blends samples under the steam atmosphere was tested by the thermogravimetric analyzer STA 449F3 (NETZSCH Company, Germany). All the experiments were performed under non-isothermal conditions at three different heating rates: 5, 10 and 20  $\text{K min}^{-1}$  from the room temperature

**Table 1**  
The chemical composition of ashes of both raw samples.

Sample	Na <sub>2</sub> O	MgO	Al <sub>2</sub> O <sub>3</sub>	SiO <sub>2</sub>	P <sub>2</sub> O <sub>5</sub>	SO <sub>3</sub>	K <sub>2</sub> O	CaO	MnO	Fe <sub>2</sub> O <sub>3</sub>
LN	1.04	1.44	14.73	65.79	0.97	6.67	1.71	4.33	0.05	2.67
SD	12.84	5.56	6.50	16.47	2.42	7.64	7.76	24.89	1.43	4.57

LN: lignite; SD: sawdust.

**Table 2**  
Proximate and ultimate analyses of the char samples.

Sample LN:SD	Proximate analysis (wt.%, db)			Ultimate analysis (wt.%, daf)				
	V	A	FC	C	H	N	S	O*
1:0	10.59	33.00	48.79	58.31	0.76	0.70	0.74	6.49
4:1	9.00	32.14	51.20	59.73	0.97	0.63	0.63	5.90
1:1	10.39	29.56	52.16	61.67	0.85	0.61	0.43	6.88
1:4	26.11	23.20	42.24	64.84	0.89	0.56	0.29	10.22
0:1	30.63	19.73	41.36	69.82	0.90	0.57	0.12	8.86

O\*: calculated by difference.

up to 1100 °C. The gasification agent used is 50 vol.% N<sub>2</sub> (99.999%) and 50 vol.% H<sub>2</sub>O. And approximately 10 mg of sample was used and the total gas flow rate is determined as 100 ml/min after several pre-experiments to ensure the experimental results reproducible. The steam generator used was ordered from Bronkhorst High-Tech, in which water was heated up to the desired temperature (453 K). Liquid and mass flow controllers were used to accurately control the flow rates of water and nitrogen in order to ensure the constant steam concentration. The buoyancy effect of TGA experiment was deducted by the initial blank experiment.

#### 2.4. Kinetic models

Kinetic parameters of the co-gasification of coal and biomass are the basic but necessary data for good design and operation of the co-gasification utility of coal and biomass. In order to acquire the reliable kinetic parameters of co-gasification of the selected typical Chinese lignite LN and biomass (i.e. SD) sawdust in this

research, different kinetics models were adopted and described in more detail as followed.

A general kinetic expression for the overall reaction rate in gas-solid reactions is written as follows (Lu and Do, 1994):

$$\frac{d\alpha}{dt} = kf(\alpha) \quad (1)$$

where  $k$  is the gasification reaction rate constant and  $f(\alpha)$  refers to the reasonable model related to the reaction mechanism. The gasification reaction rate constant is dependent on the reaction temperature and can be expressed using the Arrhenius equation, which is written as:

$$k = A \exp\left(-\frac{E}{RT}\right) \quad (2)$$

where  $A$ ,  $E$  and  $T$  are the pre-exponential factor, activation energy and temperature, respectively.

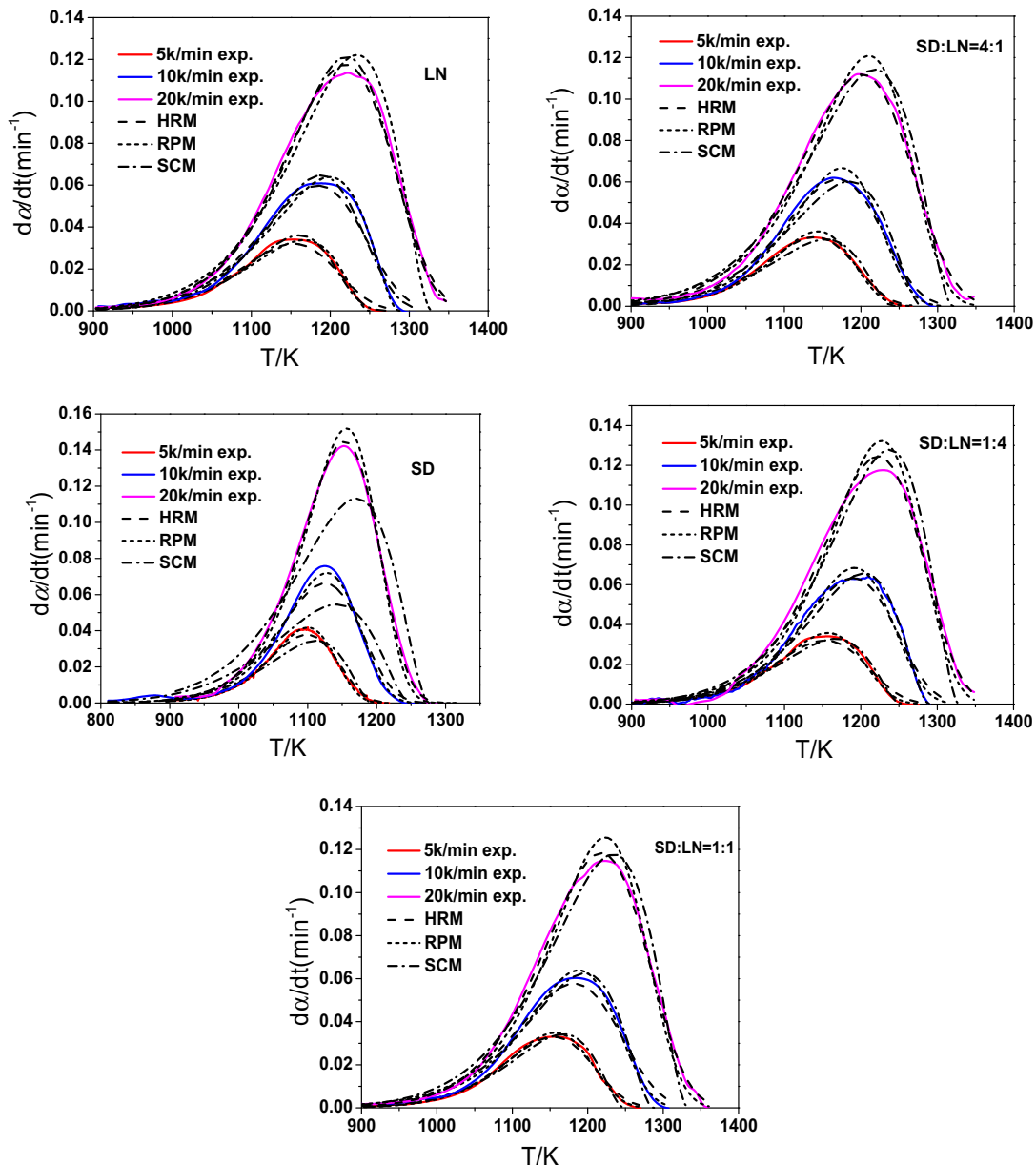


**Fig. 1.** Experimental reaction rate curves of fuel chars and those calculated with three  $n$ th-order reaction models (HRM, RPM and SCM) using parameters determined from heating rates at 5, 10 and 20 K min<sup>-1</sup>.

**Table 3**  
Initial, peak and final temperatures of gasification of lignite and sawdust.

Sample (LN:SD)	Heating rates (K min <sup>-1</sup> )	Temperature (K)			(dW/dt) <sub>max</sub> (% min <sup>-1</sup> )
		Initial	Peak	Final	
1:0	5	1069	1159	1228	1.94
4:1		1063	1157	1217	1.99
1:1		1066	1156	1214	2.04
1:4		1054	1138	1200	2.29
0:1	10	1028	1094	1147	2.84
1:0		1098	1201	1257	3.75
4:1		1095	1190	1253	4.36
1:1		1092	1185	1251	3.88
1:4	20	1079	1165	1237	4.02
0:1		1054	1122	1180	5.15
1:0		1117	1222	1293	6.43
4:1		1112	1220	1292	6.81
1:1		1111	1217	1290	6.75
1:4		1099	1202	1282	7.19
0:1		1072	1150	1214	9.12

The non-isothermal thermogravimetric method was adopted by heating the samples from the ambient to the set temperature at a constant rate  $\beta$ . The temperature,  $T$ , is increased as function of heating time,  $t$  and is written as follows:

$$T = T_0 + \beta t \quad (3)$$

where  $T_0$  is the initial temperature at which TG heating is started.

In this work, three models were applied to describe gasification of the chars studied; including the homogeneous reaction model (HRM), the random pore model (RPM) and the shrinking core model (SCM). These models give different formulations of the term  $f(\alpha)$  and described below.

The HRM supposes a homogeneous reaction throughout the char particle and a linearly decreasing reaction surface area with conversion (Ishida and Wen, 1971). The overall reaction rate is expressed by:

$$\frac{d\alpha}{dt} = kf(\alpha) = k_{HRM}(1 - \alpha) \quad (4)$$

The RPM was proposed by Bhatia and Perlmutter (Perlmutter, 2004) and widely used to characterize gasification of char, which considered the overlapping of pore surfaces during gasification and as such the area available for reaction was reduced (Bai et al., 2009). The basic equation for this model is expressed below.

$$\frac{d\alpha}{dt} = k_{RPM}(1 - \alpha)\sqrt{1 - \Phi \ln(1 - \alpha)} \quad (5)$$

where  $\Phi$  is a parameter related to the pore structure of the un-reacted sample, at which conversion  $\alpha$  is equal zero:

$$\phi = \frac{4\pi L_0(1 - \varepsilon_0)}{S_0^2} \quad (6)$$

where  $S_0$ ,  $L_0$  and  $\varepsilon_0$  represent the initial pore surface area, pore length and solid porosity, respectively.

In addition to the HRM and RPM models, the SCM model was put forward by Szekeley and Evans (1970), which supposes that a porous particle consists of an assembly of uniform nonporous grains and the reaction takes place on the surface of these grains. The space between the neighboring grains constitutes the porous network. The shrinking core behavior applies to each of these grains during the reaction. In the regime of chemical kinetic control by assuming the grains in a spherical shape, the overall reaction rate is expressed in SCM model as below:

$$\frac{d\alpha}{dt} = k_{SCM}(1 - \alpha)^{\frac{2}{3}} \quad (7)$$

After a series of transformation of Eqs. (4), (5) and (7), the corresponding conversions of these three models were expressed as followed (Fermoso et al., 2010).

$$\alpha = 1 - \exp\left(-\frac{RT^2}{\beta E} A e^{(-E/RT)}\right) \quad (8)$$

$$\alpha = 1 - \exp\left[-\frac{RT^2}{\beta E} A e^{(-E/RT)} \left(1 + \frac{\Phi}{4} \left(\frac{RT^2}{\beta E}\right) A e^{(-E/RT)}\right)\right] \quad (9)$$

$$\alpha = 1 - \left(1 - \frac{RT^2}{3\beta E} A e^{(-E/RT)}\right)^3 \quad (10)$$

Furthermore, the nonlinear least-squares method (Miura and Peter, 1989) was employed to fit the experimental data of  $d\alpha/dt$  versus temperature,  $T$ , using the three models, Eqs. 8–10. And different kinetic parameters were reached by the three different kinetic models as described above. In order to evaluate the reliability of the three kinetic models adopted in this research, the index OF was defined below (Fermoso et al., 2010).

$$OF = \sum_{i=1}^M \left( \left( \frac{d\alpha}{dt} \right)_{exp,i} - \left( \frac{d\alpha}{dt} \right)_{cal,i} \right)^2 \quad (11)$$

where  $(d\alpha/dt)_{cal,i}$  is the fitted value corresponding to the  $i$ th temperature  $T_i$ ,  $(d\alpha/dt)_{exp,i}$  is the experimental value at  $T_i$ , and  $M$  is the number of data points. In addition, the best fitting kinetic parameters were adopted by the biggest  $R^2$  value obtained from those results with statistical significance.

By comparing these two experimental and fitted  $(1 - \alpha)$  and  $d\alpha/dt$  values, the kinetic model may be further tested and verified. The error (deviation (DEV)) between the experimental and fitted curves was calculated using the following expressions by deviation (DEV) and relative error:

$$DEV(1 - \alpha)(\%) = 100 \left( \frac{\sum_{i=1}^m ((1 - \alpha)_{cal,i} - (1 - \alpha)_{exp,i}) / M}{\max(1 - \alpha)_{exp}} \right)^{1/2} \quad (12)$$

$$DEV(d\alpha/dt)(\%) = 100 \left( \frac{\sum_{i=1}^m ((d\alpha/dt)_{cal,i} - (d\alpha/dt)_{exp,i}) / M}{\max(d\alpha/dt)_{exp}} \right)^{1/2} \quad (13)$$

where  $(1 - \alpha)_{cal,i}$  and  $(1 - \alpha)_{exp,i}$  represent the fitted and experimental data of  $(1 - \alpha)$ , respectively. Similarly,  $(d\alpha/dt)_{cal,i}$  and  $(d\alpha/dt)_{exp,i}$  represent the fitted and experimental data of  $d\alpha/dt$ .  $M$

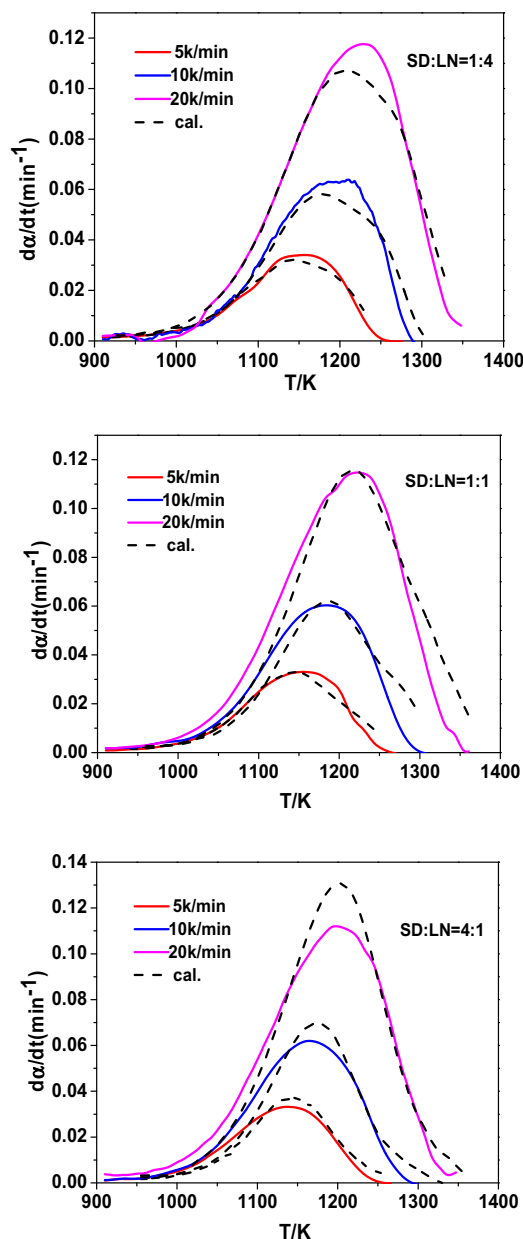


**Fig. 2.** Comparison between the experimental and calculated reaction rate curves, according to the additive rule from those of the individual components, during the non-isothermal (5, 10 and 20 K min<sup>-1</sup>) steam gasification of coal-biomass blends.

is the number of data points. And  $\max(1 - \alpha)_{exp}$ ,  $\max(d\alpha/dt)_{exp}$  are the maximal absolute values of the experimental curves.

### 3. Results and discussion

#### 3.1. Thermogravimetric characteristics of the samples under steam atmosphere

The heating rate had a marked influence on the gasification reactivity of the coal and biomass chars, independently of its nature. Fig. 1 shows the experimental reactivity data of the pure fuel chars (lignite and sawdust) and their blends by different coal-to-biomass mass ratios (1:0; 4:1; 1:1; 1:4 and 0:1), which were studied in this work as a function of reaction temperature at three different heating rates (5, 10 and 20 K min<sup>-1</sup>). Table 3 shows the initial, peak and final temperatures corresponding to the experimental reactivity plots. From Fig. 1, it could be observed that all

**Table 4**  
The maximal experimental and calculated  $d\alpha/dt$  values.

Sample (SD:LN)	Heating rate (K min <sup>-1</sup> )	Exp.		Cal.	
		$(d\alpha/dt)_{max}$ (min <sup>-1</sup> )	$T_{max}$ (K)	$(d\alpha/dt)_{max}$ (min <sup>-1</sup> )	$T_{max}$ (K)
1:4	5	0.0345	1154	0.0320	1142
	10	0.0637	1210	0.0580	1179
	20	0.1182	1230	0.1072	1208
1:1	5	0.0337	1158	0.0330	1144
	10	0.0608	1180	0.0616	1189
	20	0.1154	1220	0.1154	1220
4:1	5	0.0333	1140	0.0371	1147
	10	0.0621	1165	0.0701	1178
	20	0.1123	1201	0.1308	1203

Exp.: the experimental; Cal.: the calculated.

the curves presented a single peak and corresponds to the maximum rate of mass loss, i.e., maximum reactivity. And increase in the heating rate tiny affected the initial reaction temperature as shown in Table 3. However, from Table 3, the temperature residing at the maximum peak height was obviously moved to higher values. With the increasing heating rates, temperature increases faster and reactions involved at different stages do not have enough time to reach completion, or equilibrium, and they thus overlap with the adjacent reaction range (Lu and Do, 1994). Meanwhile, from Table 3, the gasification of the biomass chars starts at lower temperatures than that of the coal char, which indicated higher reactivity of biomass char than that of coal char. In addition, the maximum reaction rate values of sawdust gasification not only occur at lower temperatures (between 28 and 56 K) but also 2.2 and 3.4 times higher than those of the lignite char at the same heating rates. Higher gasification reactivity of sawdust than that of lignite should be attributed to the higher alkali or alkaline earth mineral contents involved in the sawdust than that of lignite, as shown in Table 3 above, which was in accordance to the observation of other workers (Di Blasi, 2009; Gómez-Barea et al., 2006; Ollero et al., 2003). For example, Doyle (Doyle, 2003) ascribed the high reactivity of biomass to a catalytic effect associated to the high alkali contents involved in the samples, especially Ca, during their combustion and gasification.

Furthermore, in the case of the steam gasification of the blends between lignite and sawdust at different mass ratios (4:1, 1:1, 1:4) shown in Fig. 1 above, the initial co-gasification temperature of the blends at the different mass ratios was slightly shifted to the lower values as compared to gasification of lignite coal alone. From Table 3, and the decreasing temperature values fall between 3 and 6 K for the 4:1 and 1:1 blends, but between 15 K for the 1:4 blend.

#### 3.2. Interactions between the components of the blends

In order to investigate whether there is the interaction between sawdust and lignite during their co-gasification, based on the experiment data of biomass and coal obtained at the same temperature, the theoretical  $d\alpha/dt$  curves were calculated by Eq. (14) below by the sum of the individual gasification behavior in the blends and presented in Fig. 2.

$$(d\alpha/dt)_{cal} = x_{LN}(d\alpha/dt)_{LN} + x_{SD}(d\alpha/dt)_{SD} \quad (14)$$

where  $(d\alpha/dt)_{LN}$  and  $(d\alpha/dt)_{SD}$  are the reaction rate of the individual fuels,  $x_{LN}$  and  $x_{SD}$  are the mass proportions of lignite and sawdust in the blend, respectively.

At the same time, the experimental  $d\alpha/dt$  curves were also provided as well to easily ascertain whether the interaction occurred or not during co-gasification of lignite with sawdust at different blends mass ratios, including 1:4, 1:1 and 4:1, respectively.



**Table 5**  
Kinetic parameters of the char samples during steam gasification determined with the temperature programmed reduction technique at three heating rates (5, 10 and 20 K min<sup>-1</sup>) for three *n*th-order reaction models.

Samples SD:LN	HRM			SCM			RPM			
	<i>E</i> (kJ/mol)	<i>K</i> (1/s)	<i>R</i> <sup>2</sup>	<i>E</i> (kJ/mol)	<i>K</i> (1/s)	<i>R</i> <sup>2</sup>	<i>E</i> (kJ/mol)	<i>K</i> (1/s)	<i>R</i> <sup>2</sup>	<i>ε</i> <sub>0</sub>
0:1	170.34	4.30E+06	0.999	152.02	3.93E+05	0.999	102.15	43.42	0.999	22.51
1:0	158.36	8.37E+05	0.999	123.94	1.01E+05	0.990	92.52	322.93	0.999	161.93
1:4	166.95	2.40E+06	0.999	149.90	5.36E+05	0.999	95.96	261.12	0.999	342.57
1:1	169.71	5.34E+06	0.999	146.86	3.25E+05	0.999	94.80	456.54	0.999	49.81
4:1	167.17	4.99E+06	0.999	137.02	1.20E+05	0.998	93.80	1008.36	0.999	35.62

HRM: the homogeneous reaction model; SCM: the shrinking core model; RPM: the random pore model.

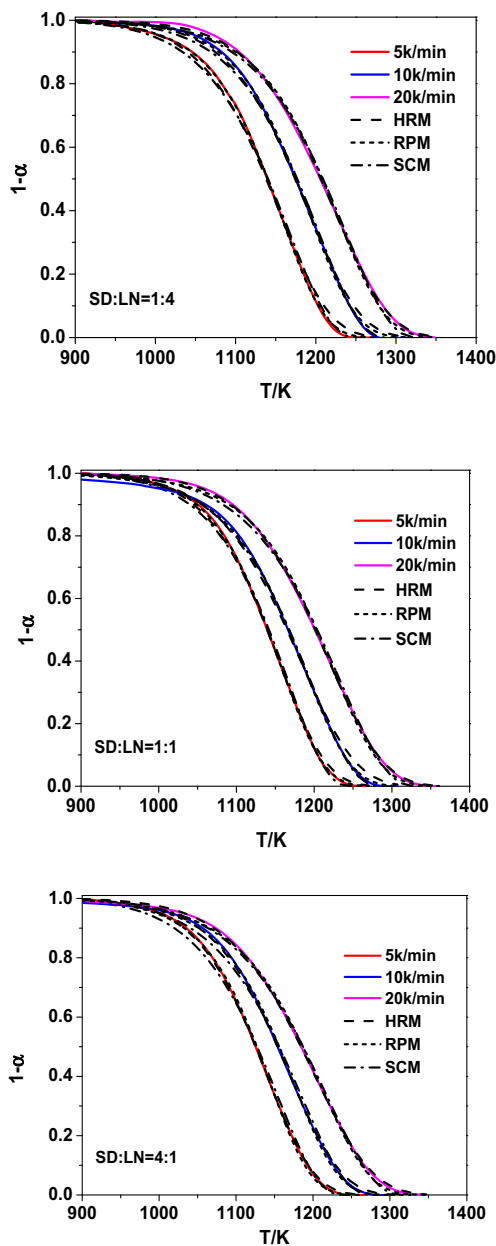


**Fig. 3.** Experimental conversion curves of fuel chars and those calculated with three *n*th-order reaction models (HRM, RPM and SCM) using parameters determined from heating rates at 5, 10 and 20 K min<sup>-1</sup>.

From Fig. 2 and Table 4 below, as the heating rate increased, both the calculated and experimental  $d\alpha/dt$  values for the lignite/sawdust blends at the different mass ratios changed as function

**Table 6**  
Deviation between the experimental and calculated conversion ( $1 - \alpha$ ) and reaction rate ( $d\alpha/dt$ ) data.

Samples SD:LN	DEV. ( $1 - \alpha$ ) (%)			DEV. $d\alpha/dt$ (%)		
	RPM	HRM	SCM	RPM	HRM	SCM
0:1	2.881	4.043	4.667	5.096	5.223	14.03
1:0	5.881	6.338	9.328	2.229	1.183	16.85
1:4	0.412	2.924	7.218	2.034	2.087	14.20
1:1	5.745	7.822	5.791	2.497	4.245	10.75
4:1	2.223	5.756	18.010	3.286	3.735	13.61

of the reaction temperature and the corresponding maximal  $d\alpha/dt$  values also increased gradually. Especially, for the sawdust/lignite blend at the mass ratio of 1:4, though the both the experimental and calculated maximal  $d\alpha/dt$  values at the different heating rates shifted to higher values, all the experimental values were larger than those calculated ones, which indicated that introduction of sawdust into lignite was much beneficial to promote the gasification reactivity of lignite for positive catalytic effect resulting from the alkali/alkaline earth content involved in the sawdust, as explained above. But the gasification behavior of the blend of sawdust/lignite at the mass ratio 4:1 was contrary to that of the blend of sawdust/lignite at 1:4, though the temperature values residing at the maximal experimental  $d\alpha/dt$  was a little lower than those temperature values at the maximal calculated  $d\alpha/dt$  values, the maximal calculated  $d\alpha/dt$  values were larger than those maximal experimental  $d\alpha/dt$  values. Such a special gasification behavior for the sawdust/lignite blend at 4:1 resulted from that more alkali minerals involved in the sawdust were introduced by overdose of sawdust in its blend with lignite and thus high gasification temperature during co-gasification resulted in agglomeration and deactivation of these alkali minerals involved in sawdust, which lowered the catalytic effect of the alkali minerals involved in the original sawdust sample. While for the sawdust/lignite blend at the mass ratio of 1:1, the maximal experimental  $d\alpha/dt$  values nearly overlapped with the calculated ones except that a little deviation between the experimental and calculated  $d\alpha/dt$  curves, which indicated there was almost no interaction between sawdust and lignite at this mass ratio during their co-gasification. Therefore, based on the co-gasification behavior presented in Fig. 2, the better mass ratio of sawdust/lignite was 1:4 for the most remarkable catalytic effect of the alkali minerals involved in sawdust functioned at this mass ratio.

### 3.3. Kinetic parameters

Finally, based on the fitted co-gasification of lignite and sawdust under a steam atmosphere using the three typical gas–solid reaction models, including HRM, RPM and SCM, the related kinetic parameters at the three different heating rates (including 5, 10 and 20 K min<sup>-1</sup>) were reached, as presented in Table 5 below.

From this Table, it could be observed that both kinetic parameter values, including  $E$ ,  $K$ , for steam co-gasification of the sawdust/lignite blends at the different mass ratios acquired from different gas–solid kinetic models fell within those kinetic parameter values for single gasification of sawdust or lignite. And the correlation coefficients  $R^2$  reached from different gas–solid kinetic models were also very close and reached above 0.99. Especially, the RPM model fits the experimental data better than the other two models for all samples, since it revealed a significant fit and has the highest  $R^2$  (0.999) value, as also validated by other workers (Kajitani et al., 2006; Okumura et al., 2009). And as to the porosity  $\varepsilon_0$  of RPM, the maximal value was reached when the mass ratio of sawdust to lignite was equal to 1:4, which implied that the positive interaction effect was better, which was in good agreement with our previous analysis.

In addition, in order to further show the fitted reliability in this research, based on the kinetic parameters reached as listed in Table 4 above, the conversion  $(1 - \alpha)$  of the chars during co-gasification was further calculated using Eqs. 8–10, as shown in Fig. 3 below. In order to quantify the errors produced by the kinetic models in predicting the values of conversion, the experimental and calculated  $(1 - \alpha)$  values were compared by calculating the deviation (DEV) between the calculated and experimental curves using Eq. (12). The same procedure was applied to the  $da/dt$  curves using Eq. (13). The related results acquired from the three different models for all the char samples are summarized in Table 6. And the lowest deviation from the calculated values was acquired using the RPM model for the sawdust, sawdust/lignite char samples at 1:4 and the HRM model for the sawdust char sample. But in relation to the calculated conversion values, the best ones were obtained using the RPM model for the lignite and sawdust/lignite 1:4 char samples and the HRM model for the sawdust/lignite char sample at 1:4. It shows again that the similarity of fit between the HRM and RPM models in the case of the sawdust/lignite 1:4 sample.

#### 4. Conclusions

Various chars were produced from lignite and sawdust and their mixtures at different mass ratios. Steam gasification reactivity of these chars were evaluated through the non-isothermal TGA analysis, which indicated that obvious interaction was found to occur between lignite and sawdust at their mass ratio of 1:4. Meanwhile, RPM was identified as the best one among all the three gas–solid models to simulate the steam-gasification behavior of the various chars prepared. Finally, rational kinetic parameters were reached and provided a good basis for design and operation of the co-gasification system using lignite and sawdust as the mixing fuel.

#### Acknowledgements

This work was supported by the National Science Foundation of China (NSFC) (Nos. 21176098, 51176062), the Research Project of Chinese Ministry of Education (No. 113045A) and the National

High Technology Research and Development of China (2012AA063504). The authors also acknowledge the extended help from the Analytical and Testing Center of Huazhong University of Science and Technology.

#### References

- Ahmed, I., Gupta, A.K., 2009. Characteristics of cardboard and paper gasification with CO<sub>2</sub>. *Appl. Energy* 86, 2626–2634.
- Arenillas, A., Rubiera, F., Pevida, C., Ania, C.O., Pis, J.J., 2004. Relationship between structure and reactivity of carbonaceous materials. *J. Therm. Anal. Calorim.* 76, 593–602.
- Bai, J., Li, W., Li, C., Bai, Z., Li, B., 2009. Influences of mineral matter on high temperature gasification of coal char. *J. Fuel Chem. Technol.* 37, 134–138.
- Barkia, H., Belkbir, L., Jayaweera, S.A.A., 2006. Kinetic studies of oxidation of residual carbon from moroccan oil shale kerogens. *J. Therm. Anal. Calorim.* 86, 121–123.
- Di Blasi, C., 2009. Combustion and gasification rates of lignocellulosic chars. *Prog. Energy Combust. Sci.* 35, 121–140.
- Doyle, C.D., 2003. Estimating isothermal life from thermogravimetric data. *J. Appl. Polym. Sci.* 24, 639–642.
- Edreis, E.M.A., Luo, G., Li, A., Xu, C., Yao, H., 2014. Synergistic effects and kinetics thermal behaviour of petroleum coke/biomass blends during H<sub>2</sub>O co-gasification. *Energy Convers. Manage.* 79, 355–366.
- Elbeyli, I.Y., Piskin, S., 2006. Combustion and pyrolysis characteristics of Tuncbilek lignite. *J. Therm. Anal. Calorim.* 83, 721–726.
- Everson, R.C., Neomagus, H.W.J.P., Kaitano, R., Falcon, R., du Cann, V.M., 2008. Properties of high ash coal-char particles derived from inertinite-rich coal: II. Gasification kinetics with carbon dioxide. *Fuel* 87, 3403–3408.
- Fermoso, J., Arias, B., Pevida, C., Plaza, M.G., Rubiera, F., Pis, J.J., 2008. Kinetic models comparison for steam gasification of different nature fuel chars. *J. Therm. Anal. Calorim.* 91, 779–786.
- Fermoso, J., Gil, M.V., Pevida, C., Pis, J.J., Rubiera, F., 2010. Kinetic models comparison for non-isothermal steam gasification of coal-biomass blend chars. *Chem. Eng. J.* 161, 276–284.
- Gómez-Barea, A., Ollero, P., Villanueva, A., 2006. Diffusional effects in CO<sub>2</sub> gasification experiments with single biomass char particles. 2. *Theor. Predictions Energy Fuels* 20, 2211–2222.
- Ishida, M., Wen, C.Y., 1971. Comparison of zone-reaction model and unreacted-core shrinking model in solid–gas reactions-I isothermal analysis. *Chem. Eng. Sci.* 26, 1031–1041.
- Kajitani, S., Suzuki, N., Ashizawa, M., Hara, S., 2006. CO<sub>2</sub> gasification rate analysis of coal char in entrained flow coal gasifier. *Fuel* 85, 163–169.
- Liu, T., Fang, Y., Wang, Y., 2008. An experimental investigation into the gasification reactivity of chars prepared at high temperatures. *Fuel* 87, 460–466.
- Long, J., Song, H., Jun, X., Sheng, S., Lun-Shi, S., Kai, X., Yao, Y., 2012. Release characteristics of alkali and alkaline earth metallic species during biomass pyrolysis and steam gasification process. *Bioresour. Technol.* 116, 278–284.
- Lu, G.Q., Do, D.D., 1994. Comparison of structural models for high-ash char gasification. *Carbon* 32, 247–263.
- Miura, K., Peter, S., 1989. Analysis of gas–solid reactions by use of a temperature-programmed reaction technique. *Energy Fuels* 3, 243–249.
- Okumura, Y., Hanaoka, T., Sakanishi, K., 2009. Effect of pyrolysis conditions on gasification reactivity of woody biomass-derived char. *Proc. Combust. Inst.* 32, 2013–2020.
- Ollero, P., Serrera, A., Arjona, R., Alcantarilla, S., 2003. The CO<sub>2</sub> gasification kinetics of olive residue. *Biomass Bioenergy* 24, 151–161.
- Perlmutter, S.K.B.A., 2004. A random pore model for fluid–solid reactions kinetic control. *Aiche J.* 26, 379–386.
- Szekely, J., Evans, J.W., 1970. A structural model for gas–solid reactions with a moving boundary. *Chem. Eng. Sci.* 25, 1091–1107.
- Wang, Q., Zhao, W., Liu, H., Jia, C., Li, S., 2011. Interactions and kinetic analysis of oil shale semi-coke with cornstalk during co-combustion. *Appl. Energy* 88, 2080–2087.
- Wu, S., Wu, Y., Gu, J., Li, L., Gao, J., 2006. The reactivity and kinetics of Yanzhou coal chars from elevated pyrolysis temperatures during gasification in steam at 900–1200 °C. *Process Saf. Environ. Prot.* 84, 420–428.
- Xu, C., Hu, S., Xiang, J., Zhang, L., Sun, L., Shuai, C., Chen, Q., He, L., Edreis, E.M., 2014. Interaction and kinetic analysis for coal and biomass co-gasification by TG-FTIR. *Bioresour. Technol.* 154, 313–321.